Jurnal Polimesin
Department of Mechanical Engineering
State Polytechnic of Lhokseumawe
http://e-jurnal.pnl.ac.id/polimesin

e-ISSN	: 2549-1999	No.	: 1	Month	: February
p-ISSN	: 1693-5462	Volume	: 23	Year	: 2025

Processing dates: received on 2024-08-07, reviewed on 2024-11-11, accepted on 2024-11-29 and online availability on 2025-02-28

Finite element analysis of wear and deformation in casing rings for centrifugal pumps

Susilo Handoko*, Regan Rahadian P, Hafid Suharyadi, Totok Widiyanto
Refinery of Mechanical Engineering, Akamigas Polytechnic of Energy and Mineral, Cepu 58315, Indonesia
*Corresponding author: susilohandoko65@gmail.com

Abstract

The wear and deformation of critical components in centrifugal pumps, such as wear-casing rings, can be caused by the influence of operational lifetime and varying boundary conditions. To enhance the accuracy of wear and deformation predictions, this study integrates finite element analysis (FEA) with detailed field measurement data, including material wear rates and load conditions. The boundary conditions were applied to the (Computer Aided Design) CAD model of the wear-casing ring under varying operational loads. The simulation results indicate that the wear casing ring experiences a maximum deformation of 0.0037545 mm, with an estimated lifespan of 5.571×10^7 cycles under normal loading and 0.5517×10^7 cycles under doubled loading conditions. The installation clearance of the wear casing ring is 0.38 mm, with a tolerance of 0.05 mm. The deformation results fell within the acceptable limits for continued use, meeting the clearance standard. The contributions of this study lie in providing more precise wear predictions and insights into wear ring performance and an applicable predictive maintenance method that can be used to improve pump reliability and reduce maintenance costs.

Keywords:
wear casing ring, clearance, deformation, finite element analysis, lifetime, centrifugal pump.

1 Introduction

Centrifugal pump is a rotating equipment used to add energy and increase the kinetic energy of the fluid by using a prime mover and an impeller. [1] Pump failures are frequent. [1]–[3] The failure of its components may cause a short lifetime of the centrifugal pump, selection errors in materials [4], [5], design errors from the manufacturing process [1], [4], manufacturing defects [1], [2], [4], and lack of consistency in maintenance. Fluid leakage, bearing fatigue, impeller defects, component tears, and coupling fatigue are the most common failures occurring in centrifugal pumps [1], [2], [4], [6], [7].

The wear casing ring was inserted into the pump casing. It is essential that the clearance between the wear casing ring and the wear impeller ring is neither too tight nor too loose. A tight clearance can generate heat due to friction between the outer surface of the wear impeller ring and the inner surface of the wear casing ring, leading to potential overheating. Conversely, if the clearance is too loose, internal pressure loss may occur, which can further decrease the operational efficiency of the pump. Therefore, maintaining the appropriate clearance is crucial for optimal performance [1], [7] [8]. Fig. 1. shows the least tolerable clearance between the wear ring components [1]–[3], [5], [9]–[15][16]. After running for a certain working cycle, the wear ring casing will most likely experience a defect on the outer surface of the wear ring, thus forming a gap and wear that will cause internal pressure loss. Fig. 2. shows the defect and wear of the wear ring after two weeks of usage [1].

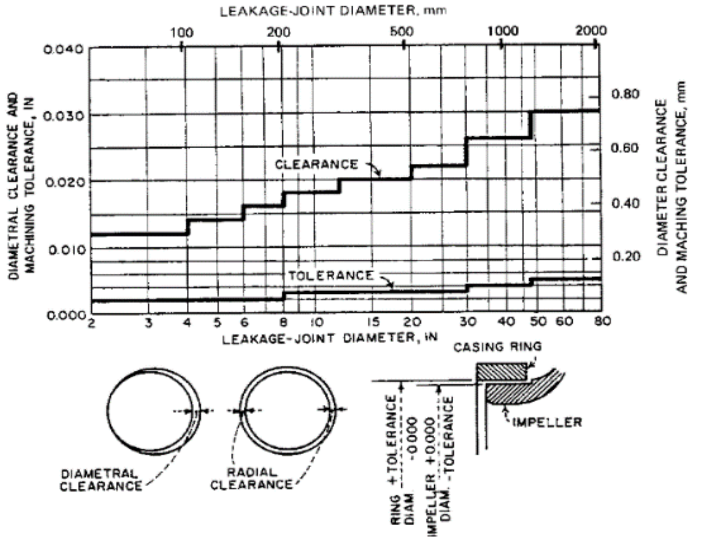

Fig. 1. Minimum clearance between the wear ring impeller and wear casing [16].

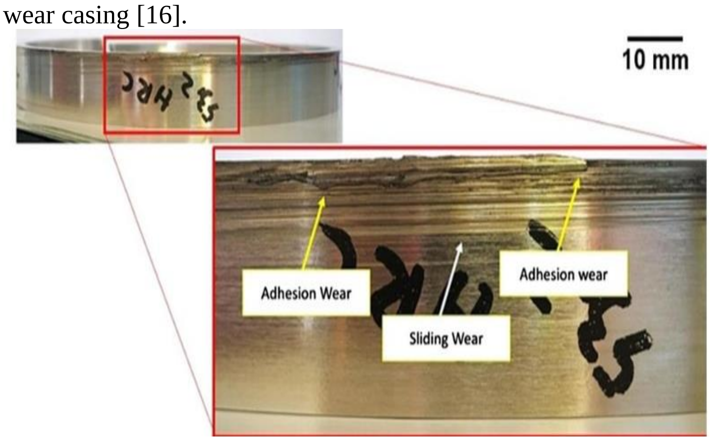

Fig. 2. Defects on outer surface of wear ring impeller [1]

Finite Element Analysis (FEA) is a computational technique employed to simulate and approximate complex engineering problems under specific boundary conditions. The results obtained from FEA serve as valuable parameters in the design and modelling of physical engineering materials, whether solid, liquid, or gaseous. This method relies heavily on the discretization of the model into numerous nodes and elements. The approximate solution is then constructed using weighted residual methods alongside mathematical approaches. [17], [18] This computational approach can be used to determines the deformation of the wear casing ring thus can be used as a guidance on the clearance of the wear casing ring usage, this deformation can be further analyze to know the fatigue of the wear casing ring [5], [9], [14].

The ANSYS® Mechanical Student version, a general-purpose finite element analysis software, was employed for the analysis. This computational approach enables the assessment of wear ring defects and deformation over a specified lifetime through a simulation model grounded in defined boundary conditions.

The wear and deformation of the critical components in centrifugal pumps, such as wear rings, have been extensively studied in the existing literature [1], [4]. Prior research has predominantly focused on generalized failure modes or standard operational conditions, often neglecting the influence of operational lifetime and varying boundary conditions. Such gaps limit the applicability of these studies in predicting real-world performance. This research addresses this limitation by integrating detailed field measurement data, such as material wear rates and load conditions, with FEA. This approach not only enhances the accuracy of wear and deformation predictions but also provides actionable insights into the operational lifecycle of wear rings under diverse loading conditions, improving pump reliability and reducing maintenance costs.

2 Method

This research employed a quantitative approach, utilizing ANSYS Mechanical as a computational tool to analyze wear ring defects and deformation over a specific lifetime under defined boundary conditions. The methodology began with an overhaul process, during which wear casing ring component data were measured to ensure accurate input parameters for computational modeling.

The data were processed and transformed into a Computer-Aided Design (CAD) model to accurately represent the geometry of the wear ring. This model was subsequently prepared for FEA by defining the mesh, material properties, and boundary conditions based on field data. Using ANSYS Mechanical, the study simulated the deformation of the wear ring and evaluated its remaining operational life under applied loads. [17], considering both static and dynamic factors. Finally, the results of the computational analysis were validated against field data from real-world examples [1], ensuring that the findings were consistent with practical performance and conditions.

The dimensions of the wear ring model taken from the measuring dimensions of the EBARA® centrifugal pump wear rings are shown in Figs 3 and 4, which can be seen in Tables 1 and 2.

Tables 1 and 2 present the dimensions of each wear-casing component in the analyzed centrifugal pump. These dimensions were measured meticulously during the overhaul process to ensure accuracy. The properties listed in these tables are essential for modeling the wear casing ring in the CAD software, forming the foundation for subsequent simulations. The CAD model, developed using these precise dimensions, was analyzed using ANSYS Mechanical Student Edition to evaluate deformation and wear patterns under varying operational conditions.

Fig. 3. EBARA Wear Casing Ring

Table 1. EBARA Wear Casing Ring

Wear Casing Ring	Values
Inside Diameter (ID)	111.95 (mm)
Outside Diameter (OD)	121.5 (mm)
Thickness	20 (mm)
Weight	150 (grams)

Table 2. EBARA Wear Impeller Ring

Wear Casing Ring	Values
Inside Diameter (ID)	122.5 (mm)
Outside Diameter (OD)	137.5 (mm)
Thickness	20 (mm)
Weight	200 (grams)

Fig. 6(a) shows the modeled CAD wear casing ring using ANSYS Discovery based on the dimensions given in Table 1. Table 3. provides the physical parameters of the material used for the wear ring, which was made of structural steel.

Fig. 4. EBARA Wear Impeller Ring

The material properties, such as yield strength, tensile strength, and modulus of elasticity, were derived from the 1998 ASME Boiler and Pressure Vessel Code (BPV), Section 8, Division 2, Table 5-110.1 [13] [19]. These values were critical for ensuring the accuracy of the finite element analysis conducted using ANSYS Mechanical. Additionally, the fatigue behavior of the material was evaluated using the fatigue curve (S-N Curve) shown in Fig. 5. This curve [13] [19], showing the relationship between stress amplitude and the number of cycles to failure. The data in Table 3 and the curve in Fig. 5 were integral to predicting the wear ring lifespan under cyclic loading conditions.

Table 3. Structural Steel Physical parameters

Material Properties	Values (units)
Elastic Modulus	200 (GPa)
Density	7850 (Kg/m^3)
Poisson's ratio	0.3
Yield strength	250 (MPa)
Behavior	Isotropic

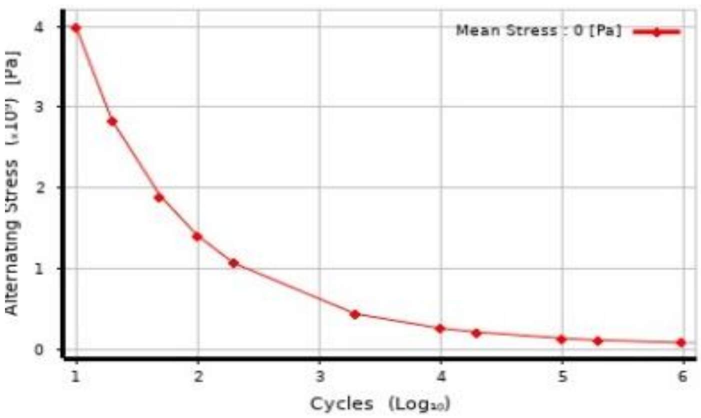

Fig. 5. Structural Steel S-N Curve

To evaluate deformation and displacement, the nodes representing the initial shape coordinates were defined as boundary conditions, allowing the model to deform under applied loads. Body sizing was employed as the meshing option for the wear ring to ensure accurate analysis. The generated mesh comprised 138 elements and 1,130 nodes, as shown in Fig. 6(b) and Fig. 6(c). [17]. The boundary conditions for the analysis were established based on the data presented in Table 4, whereas the load conditions were defined according to Table 5. These parameters were derived from the operational performance of the centrifugal pump during its running condition, ensuring that the simulation accurately reflects real-world scenarios [17].

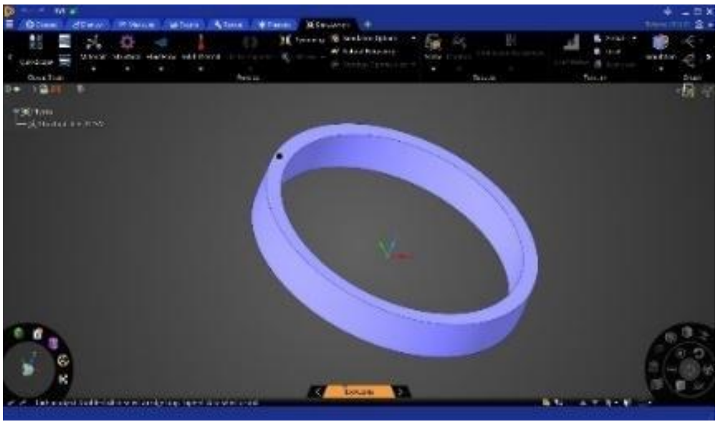

(a) Ring CAD Model

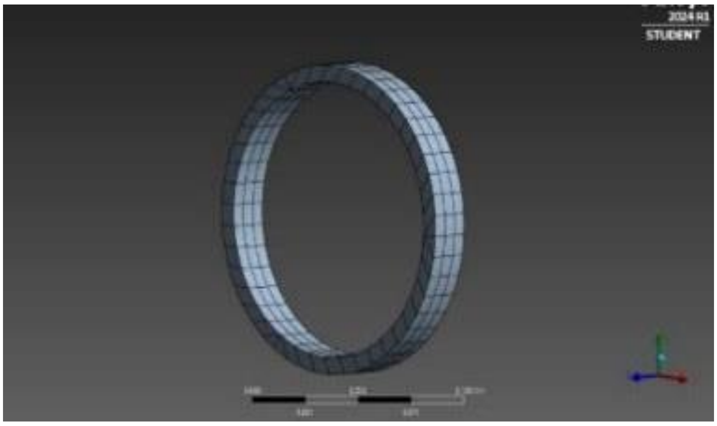

(b) Ring Mesh

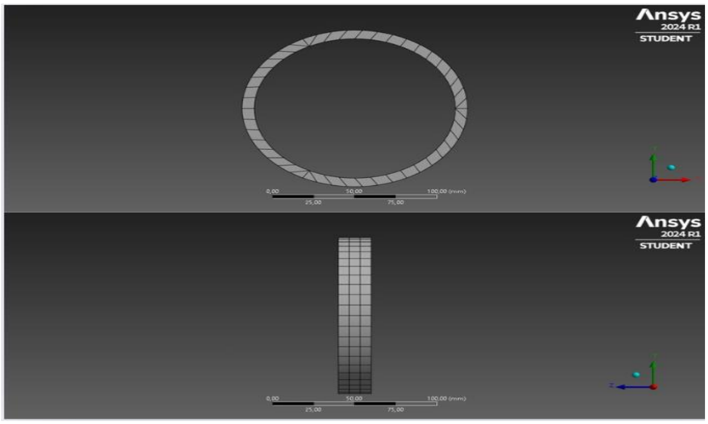

(c) Ring Mesh (X, Y) (Z, Y)

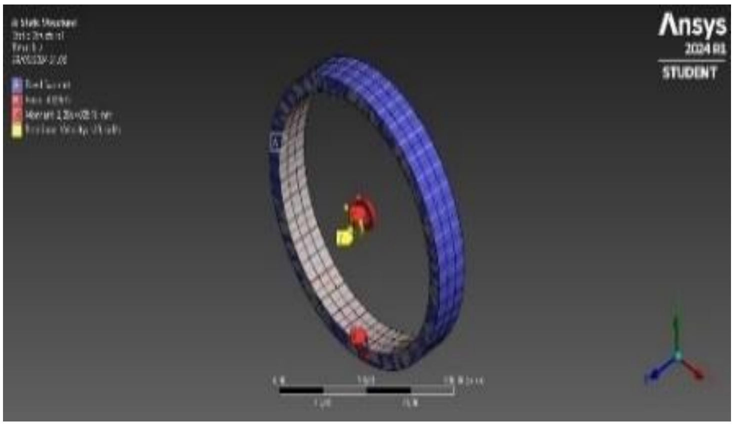

(d) Boundary and Load Condition

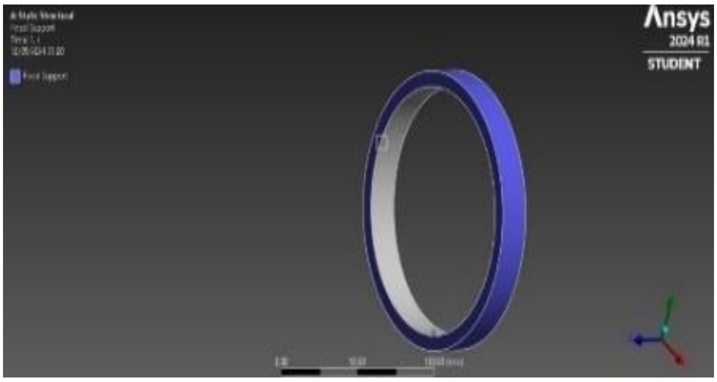

(e) Fixed Support

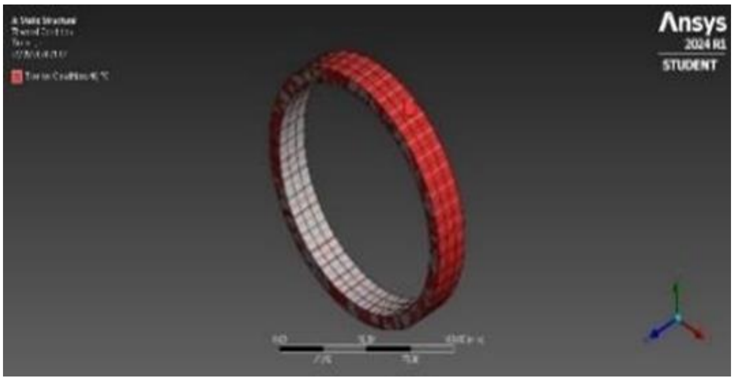

(f) Thermal Condition

Fig. 6. Wear casing

Table 4. Wear Ring Boundary Condition Given

Boundary Condition	Values (units)
Fixed support	2 (Faces)
Thermal condition	40° (°C)

Fig. 6(d). shows the positioning of the wear casing ring within the pump casing, along with the applied load conditions. The load conditions are designed to approximate the moments and forces acting on the wear casing ring during the operation of the pump impeller. These conditions are defined based on the operational performance of the pump, as detailed in Table 5., which outlines the load applied to the wear casing ring, including the moments from the motor and the forces exerted by the impeller.

Table 5. Wear Ring Load Condition Given

Load Condition	Values (units)
Force load (-Y Axis)	49.89 (N)
Moment	209e+005 (N.mm)
Rotational velocity	298 rad/s

The boundary-condition values are listed in Table 4., specify the temperature of the circulating fluids and the interaction surfaces between the wear casing ring and centrifugal pump volute, which can be further seen in Fig. 6€. and Fig. 6(f).

1. Fixed support of the wear ring. The fixed support is set on geometric faces in which the geometry is static (facing the casing).
2. Thermal condition of the wear ring. The thermal condition is set to be ambient (40 °C)The load condition was obtained from this equation.
3. Force load given to the wear ring (N). The force load applied to the wear ring is obtained from the weight of the impeller and impeller wear ring using the Eq. (1) [20].
   $F = ma$
   $$kgf\ (N) = kg\ x\ F \qquad (1)$$
4. Moment given to the wear ring (N.mm). Fig. 7. shows the relation between the torque of the pump based on the speed given by the motor, this is used to determines the amount of moment load given to the wear ring based on the rpm of the centrifugal pump motor. The resulting moment is converted from an imperial unit to a metric unit, and a conversion factor is used Eq. (2).

$$1\ lbf.ft = \ 1355.818\ kgf.mm \qquad (2)$$

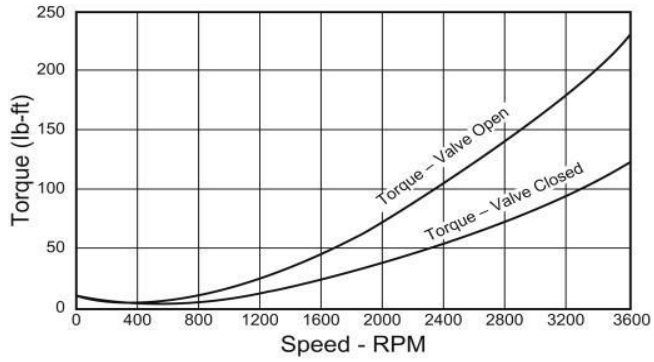

Fig. 7. Torque vs Speed Graph [21]

5. Rotational velocity given to the wear ring (rad/s).To convert the rotational velocity from revolutions per minute (rpm) to radians per second (rad/s), a conversion factor is used Eq. (3) [22].

$$\omega = \frac{2\pi \times n}{60} \quad (3)$$
$$\omega = \frac{2\pi \times 1\,rpm}{60}$$
$$\omega = 0.1047\,rad/s$$

Based on the boundary condition and load condition given on the wear casing ring, the simulation then can be done by choosing the desired analysis settings within the ANSYS Mechanical software

The analysis chosen in this analysis were equivalent stress, total deformation and fatigue tool. Within the fatigue tool in the solution tab, life, damage, safety factor, biaxiality indication, and fatigue sensitivity were set as the desired solution within the ANSYS Mechanical software. Fig. 8. The solution tab chosen for the software is presented.

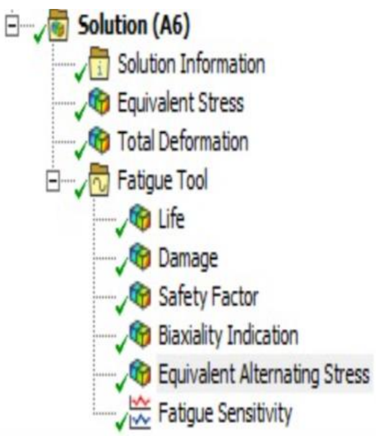

Fig. 8. ANSYS solution tab

3 Results and Discussion

3.1 ANSYS simulation result

Based on the loads specified in Table 5 and the boundary conditions outlined in Table 4, the analysis was performed using ANSYS Mechanical Student software. The results included the total deformation of the wear casing ring and the equivalent stress under the applied loads. Equivalent stress is a crucial parameter for assessing the wear casing ring's life, damage, and safety factors based on the selected material. The damage associated with equivalent stress was further evaluated through biaxiality indication analysis. Additionally, fatigue sensitivity was assessed to determine the remaining lifespan of the wear casing ring as a function of the applied load cycles. The variables are:

1. **Total Deformation**

Total deformation represents the change in size due to wear and defects in the wear casing ring. The magnitude of this deformation as in Table 6, with an average wear casing ring deformation of 0,0012115 mm. Fig. 9(a) presents the heat map of the deformation in the isometric plane, whereas Fig. 9(b) shows the deformation along the Z- and Y-axes. As shown in Fig. 9(b), the wear casing ring tends to move outward owing to the applied internal load. This deformation is consistent with the findings of [1], where the internal deformation causes material to move outward, resulting in an increase in the wear casing ring clearance.

Table 6. Wear Ring Total Deformation Result

Taken Deformation	Deformation (mm)
Maximum	0.0037545
Average	0.0012115
Minimum	0

1. **Equivalent Stress (von mises stress)**

The equivalent stress represents the maximum stress endured by the wear casing ring. The equivalent stress values are based on the applied load parameters listed in Table 5. The magnitude of the stress experienced by the ring varied depending on the critical points within the wear-casing ring. This result as in Table 7. The maximum stress taken by the wear casing ring is 124.8 MPa, which influences the deformation and other factors affecting the wear casing ring. The stress distribution is shown in the heat map in Fig. 9(c).

Table 7. Wear Ring Equivalent Stress Result

Taken Stress	Stress (MPa)
Maximum	124.8
Minimum	4.8977

2. **Life**

Life represents the total number of cycles that a wear ring can endure before fracturing or sustaining significant damage. The lifespan of the wear ring, as illustrated in Fig. 5, is directly influenced by the equivalent stress experienced by the material. Based on the provided parameters, the maximum estimated lifespan of the wear ring is 3.8052×10^8 cycles, reflecting its performance under specified load and boundary conditions. Additionally, the heatmap in Fig. 9(d) illustrates the distribution of the wear casing ring's lifespan, emphasizing areas of potential stress concentration. This data serves as a valuable baseline for implementing effective preventive maintenance strategies for wear casing rings. [1]

3. **Damage**

Damage quantifies the degree of material degradation in the wear ring resulting from applied loads and boundary conditions. It is represented as a damage factor that measures the accumulation of wear and fatigue over the material's operational life. The analysis identified a maximum damage factor of 17.949 for the wear ring, indicating significant stress levels that bring the material closer to its failure threshold. The damage factor is influenced by the equivalent stress distribution and the material properties under cyclic loading; higher stress concentrations contribute to increased damage. Critical regions, often located near load application points or geometric discontinuities, are essential for monitoring to ensure effective preventive maintenance. [1]. The damage distribution is shown as a heat map in Fig. 9 (e). highlights the areas that are most susceptible to failure.

4. **Safety factors**

The safety factor is defined as the ratio of a material's strength to the applied stress, providing a measure of the safety margin before failure. For the wear ring, the calculated minimum safety factor, based on the specified parameters, is 0.69072. This value indicates that the wear ring operates near its failure threshold under the given loading conditions. A safety factor below 1 suggests that the material may not endure the applied loads over extended periods, thereby increasing the risk of structural failure. The distribution of safety factors is illustrated in the heatmap presented in Fig. 9(f), which highlights critical regions with lower safety margins—often associated with areas of high stress concentration. This information is essential for evaluating operational limits and informing design or maintenance strategies to enhance the reliability of the worn casing ring.

5. Biaxiality indication

The biaxiality indication represents the ratio of the principal stresses at any given point, providing insight into the stress state of the material. For the wear ring, the maximum biaxiality indication was 0.99175 and the minimum was -0.64277, reflecting varying stress conditions across the ring. Positive values indicate tensile stresses in multiple directions, whereas negative values indicate a combination of tensile and compressive stresses. Fig. 9(g). presents the biaxiality heatmap, highlighting regions where stress interactions are most critical. These values help identify potential weak points that may require closer inspection or design adjustments.

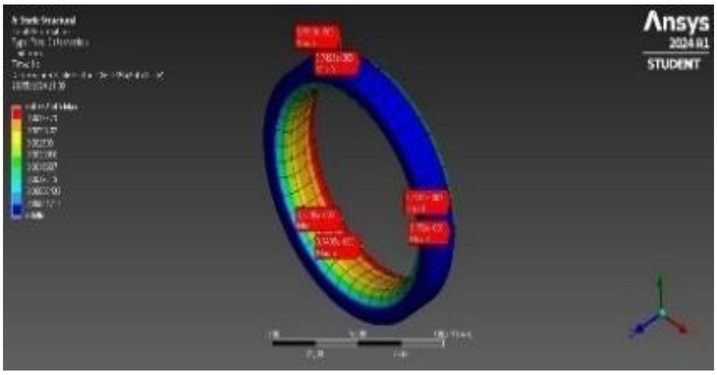

(a) Total deformation

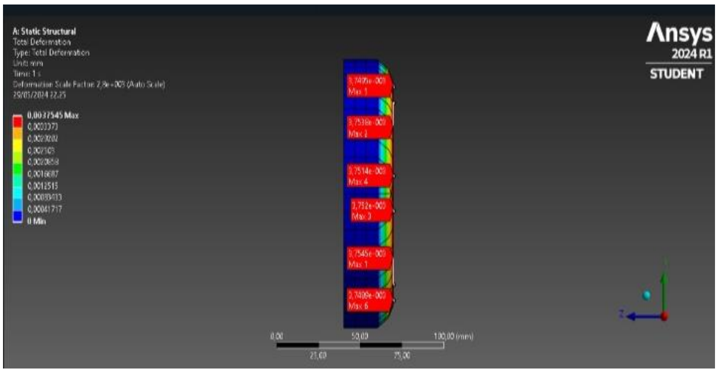

(b) Deformation (Z, Y)

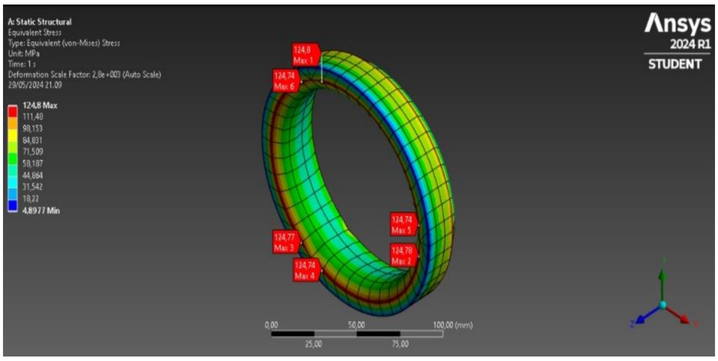

(c) Equivalent stress

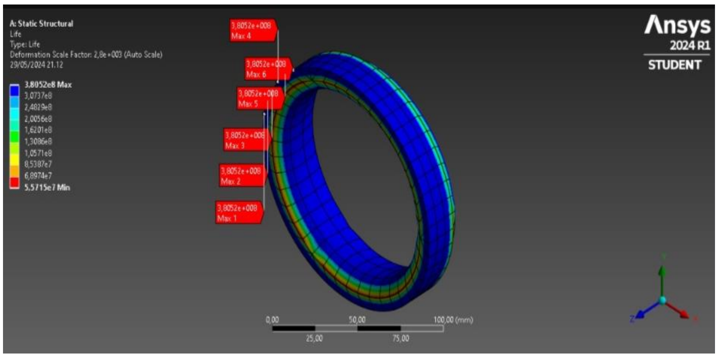

(d) Wear ring life

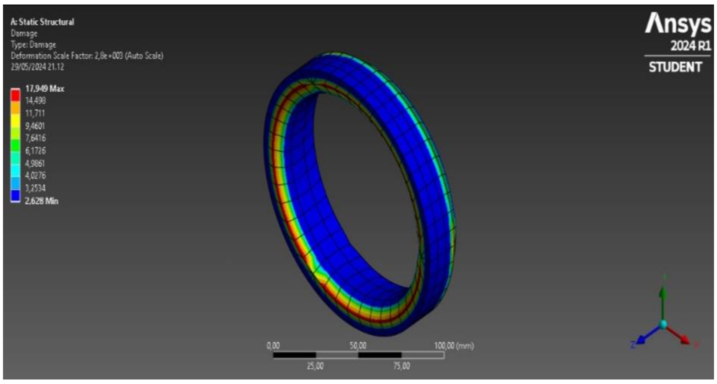

(e) Damage

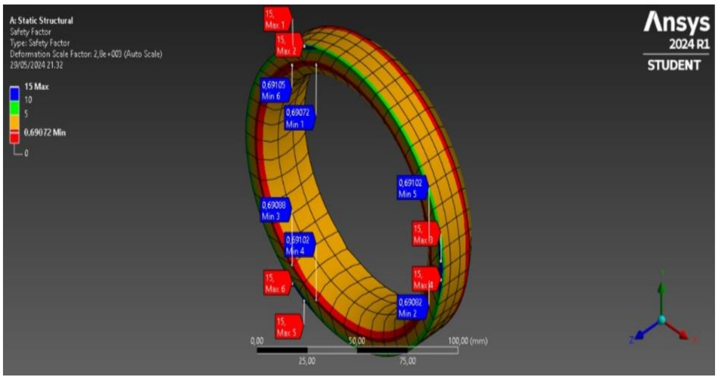

(f) Safety factors

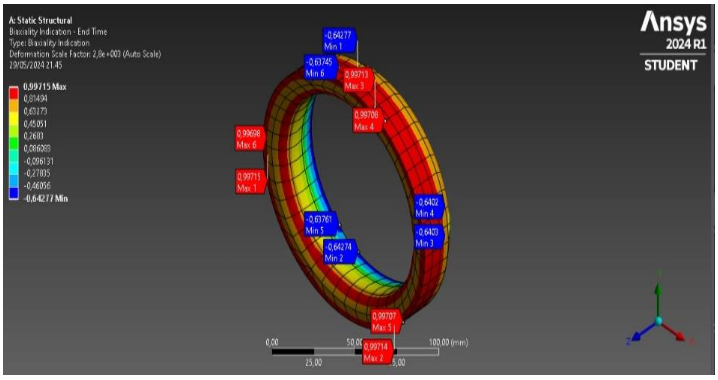

(g) Biaxiality Indication

Fig. 9. Wear ring

6. **Fatigue sensitivity**

The fatigue sensitivity represents the susceptibility of the wear ring to fatigue failure under repeated loading cycles. This highlights the impact of variations in the loading history on the ability of the material to endure cyclic stress. The fatigue sensitivity of the wear-casing ring is shown in Fig. 10., indicating critical areas in which cyclic loading may accelerate wear or damage. This analysis helps identify regions at higher risk of fatigue failure, aiding in the design and maintenance planning to extend the component's operational lifespan [1].

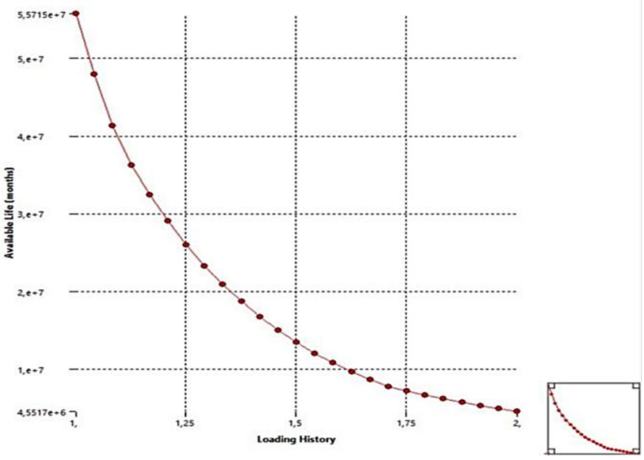

Fig. 10. Fatigue Sensitivity Graph

3.2. Displacement Analyzation Result

The maximum deformation of the casing wear ring with the given load and boundary condition was 0.3762455 mm which as listed in Table 7. Based on Fig. 1, the maximum clearance of a wear ring with an outside diameter of 121.5 mm is 0.38 mm and a tolerance of 0,05 mm which as in wear ring clearance toleration: clearance is 0.38 mm, tolerance is 0.05 mm, and clearance tolerance is 0.33 mm (min) – 0.43 mm (max). The maximum and minimum deformations of the wear ring are listed in Table 8 and can be obtained using the Eq. (4). The lifetime of the wear-casing ring with increasing load as in Table 9.

$$\Delta\emptyset\ Wear\ Ring = Clearance - \ Deformation \quad (4)$$

Table 8. Wear ring clearance deformation

Wear Ring Deformation (mm)	Wear Ring Clearance (mm)	Wear Ring Clearance After Deformation (mm)
0.0037545 (Maximum)	0.38	0.3762455
0.0012115 (Average)	0.38	0.378885
0 (Minimum)	0.38	0

Table 9. Wear ring available life

Available Life (Month x10^7)	Load (Times)
5.571	1×
2.7	1.25×
1.5	1.5×
0.8	1.75×
0.5517^7	2×

Based on the above results, the available life of the wear ring decreases by up to × 10^{-1} months when the load is increased by 2× (times) the load on the wear ring. The deformation resulting from a 1× (times) load applied to the wear casing ring can be compared with the clearance tolerance to determine the usability of the wear ring, as shown in Table 10.

Table 10. Wear ring clearance deformation

Clearance Toleration	Wear Ring Clearance After Maximum Deformation	Result Compatibility with Tolerance
0.43 mm (max)	0.3762455 mm	Acceptable (<0.43 mm)
0.33 mm (min)		Acceptable (>0.33 mm)

The results show that the deformed wear casing ring is still compatible and meets the tolerance for further usage with an approximate life of 5.571 × 10^7 (Months). This result does not include other wear and deformation variables such as corrosion and the sudden heat change of the wear ring.

Wear and deformation wear rings have been extensively studied in the existing literature [1], [4]. with results focusing on the damage and microstructure of the wear-casing ring parts without testing various loads and varying boundary conditions to further increase the operational lifetime. Such gaps limit the applicability of these studies in predicting real-world performance. This result shows the available life of the wear ring based on the given load while also helps determine whether the wear ring clearance meets the standard specifications, ensuring the pump operates within acceptable tolerance with reliable operation and reduction in maintenance time and cost.

4 Conclusion

Based on the simulation results of the wear casing ring with an outside diameter of 121.5 mm and an inside diameter of 111.95 mm, under the given boundary and load conditions, the maximum deformation of the wear ring is 0.0037545 mm. The wear ring's lifespan is estimated to be 5.571 × 10^7 cycles under normal loading and 0.5517 × 10^7 cycles under a doubled load, indicating a decrease of approximately 10% in lifespan when the load is increased. The installation clearance of the wear casing ring is 0.38 mm, with a tolerance of 0.05 mm, as shown in Fig. 1. The maximum deformation at one time load is 0.3762455 mm, which is acceptable for continued use and meets the standard tolerance for wear ring clearance. For future work, a more in-depth Computational Fluid Dynamic (CFD) analysis could enhance the accuracy of the deformation predictions, particularly by examining how the flow regime, such as cavitation, affects wear and damage to the wear casing ring, providing valuable insights into the ring's performance and longevity under different operating conditions.

References

[1] E. Pujiyulianto, A. Muhyi, F. Paundra, F. Perdana, H. T. Yudistira, and M. Syaukani, “Failure analysis of a wear ring impeller,” Eng. Fail. Anal., vol. 138, p. 106415, 2022, doi: 10.1016/j.engfailanal.2022.106415.

[2] G. Peng, Q. Chen, L. Bai, Z. Hu, L. Zhou, and X. Huang, “Wear mechanism investigation in a centrifugal slurry pump impeller by numerical simulation and experiments,” Eng. Fail. Anal., vol. 128, pp. 1–13, 2021.

[3] G. Peng, F. Fan, L. Zhou, X. Huang, and J. Ma, “Optimal hydraulic design to minimize erosive wear in a centrifugal slurry pump impeller,” Eng. Fail. Anal., vol. 120, pp. 1–13, 2021.

[4] R. Yu and J. Liu, “Failure analysis of centrifugal pump impeller,” Eng. Fail. Anal., vol. 92, pp. 343–349, 2018.

[5] A. K. Sheikh, M. Younas, and D. M. Al-Anazi, “Weibull analysis of time between failures of pumps used in an oil refinery,” in The 6th Saudi Engineering Conference, Dhahran, 2002.

[6] Samotics, “Top 5 failures in pumps and how to detect them.” 2020. [Online]. Available: https://www.samotics.com/top-5-failures-in-pumps-and-how-to-detect-them

[7] B. P. Heinz and F. K. Geitner, Machinery Failure Analysis and Troubleshooting. Woburn: Butterworth-Heinemann Publishing Company, 1997.

[8] H. P. Bloch, Machinery Lubrication. Noria, 2011. [Online]. Available: https://www.machinerylubrication.com/Read/28467/pump-failure-analysis

[9] A. R. Al-Obaidi, “Investigation of effect of pump rotational speed on performance and detection of cavitation within a centrifugal pump using vibration analysis,” Heliyon, vol. 5,

no. 6, p. e01910, 2019, doi: 10.1016/j.heliyon.2019.e01910.
[10] S. Hariady, "Analisa Kerusakan Pompa Sentrifugal 53-101C WTU Sungai Gerong PT. Pertamina RU III Plaju," J. Desiminasi Teknol., vol. 2, no. 1, 2014.
[11] R. Bhandari, "A Maintenance Report on Centrifugal Pump." 2022.
[12] W. Chaowei, L. Peng, C. Boren, and Z. Xingpan, "Design of pump fault diagnosis system based on T-FMEA," in IOP Conference Series: Journal of Physics: Conference Series, 2018.
[13] L. MatWeb, "Online materials information resource." https://www.matweb.com/
[14] W. Finnegan, Y. Jiang, N. Dumergue, P. Davies, and J. Goggins, "Investigation and Validation of Numerical Models for Composite Wind Turbine Blades," J. Mar. Sci. Eng., vol. 9, p. 525, 2021, doi: 10.3390/jmse9050525.
[15] J. Riegel, W. Mayer, and Y. V Havre, "FreeCAD." [Online]. Available: http://www.freecadweb.org
[16] I. J. Karassik, J. P. Messina, P. Cooper, and C. C. Heald, Eds., Pump Handbook, 4th ed. New York: McGraw-Hill, 2008. [Online]. Available: https://www.accessengineeringlibrary.com/content/book/9780071460446
[17] R. K. Patel, "Fatigue and Modal Analysis of Crankshaft Using ANSYS Software," 2019.
[18] A. Muhammad and I. H. Shanono, "Transient Analysis And Optimization Of A Knuckle Joint," Kinet. Game Technol. Inf. Syst. Comput. Network, Comput. Electron. Control, vol. 4, no. 2, pp. 179–186, 2019, doi: 10.22219/kinetik.v4i2.767.
[19] BPVC Section VIII-Rules for Construction of Pressure Vessels Division 1. New York, NY, USA: ASME, 2023.
[20] Y. A. Çengel and A. J. Ghajar, Heat and Mass Transfer: Fundamentals and Applications, 5th ed. New York, NY, USA: McGraw-Hill Professional, 2014.
[21] E. W. McAllister, Pipeline Rules of Thumb Handbook, 8th ed. Gulf Professional Publishing, 2014. doi: 10.1016/B978-0-12-387693-5.00014-0.
[22] A. Thompson and B. Taylor, Guide for the Use of the International System of Units (SI). Gaithersburg, MD: National Institute of Standards and Technology, 2008. doi: 10.6028/NIST.SP.811e2008.